# STUDY OF THE PROPERTIES OF BIOTIN-STREPTAVIDIN SENSITIVE BIOFETS

Thomas Windbacher, Viktor Sverdlov, Siegfried Selberherr
*Institute for Microelectronics, TU Wien, Gußhausstraße 27–29/E360, A-1040 Wien, Austria*
*Windbacher@iue.tuwien.ac.at, Sverdlov@iue.tuwien.ac.at, Selberherr@iue.tuwien.ac.at*

Clemens Heitzinger, Norbert Mauser
*Wolfgang Pauli Institute and Department of Mathematics, University of Vienna, Nordbergstrasse 15, A-1090 Wien, Austria*
*Clemens.Heitzinger@univie.ac.at, Norbert.Mauser@univie.ac.at*

Christian Ringhofer
*Department of Mathematics, Arizona State University, Tempe, AZ 85287, U.S.A.*
*Ringhofer@asu.edu*

Keywords: BioFET, Field-effect biosensor, Biotin-streptavidin, Simulation, Multi-scale problem, Interface conditions.

Abstract: In this work the properties of a biotin-streptavidin BioFET have been studied numerically with homogenized boundary interface conditions as the link between the oxide of the FET and the analyte which contains the biosample. The biotin-streptavidin reaction pair is used in purification and detection of various biomolecules; the strong streptavidin-biotin bond can also be used to attach biomolecules to one another or onto a solid support. Thus this reaction pair in combination with a FET as the transducer is a powerful setup enabling the detection of a wide variety of molecules with many advantages that stem from the FET, like no labeling, no need of expensive read-out devices, the possibility to put the signal amplification and analysis on the same chip, and outdoor usage without the necessity of a lab.

## 1 INTRODUCTION

Today's technology for detecting tumor markers, antigen-antibody complexes, and pathogens is time-consuming, complex, and expensive (Pirrung, 2002), (Shinwari et al., 2006). For instance, a typical procedure to detect a given DNA complex is to increase the concentration by RT (reverse transcription) or PCR (polymerase chain reaction), followed by a process step that will add a label to the DNA enabling detection by light or radiation. After all these steps the sample is applied to a microarray. The microarray consists of an array of spots, and every single spot is able to detect a different type of molecule. After the reaction has taken place the array is read by an expensive microarray reader.

Replacing the above sensing mechanism by an electrical detection has several benefits. First, the optical microarray reader becomes superfluous. Detection by FET (field-effect transistor) makes the integration of amplifying and analyzing circuits on the same chip possible, thus saving also equipment. The advanced development of semiconductor process technology allows mass production of such devices, decreasing the price dramatically. Various kinds of reaction pairs are possible and have been studied, like detection of DNA (Fritz et al., 2002), (Hahm and Lieber, 2004), (Gao et al., 2007), cancer markers (Zheng et al., 2005), proteins, e.g. biotin-streptavidin (Im et al., 2007), (Cui et al., 2001), (Gupta et al., 2008), (Stern et al., 2007), albumin (Park et al., 2008), and transferrin (Girard et al., 2006). In these papers different device types and materials were investigated and provided different solutions for each problem. In principle, every molecule that is charged in the solute and that can be bound to the surface layer can be detected by a BioFET. The field of applications is very wide and spans from DNA sequencing, point of care applications, to controlling environmental pollution and the spread of diseases. The BioFET can be easily integrated into the chip environment. By putting a microfluidic channel above the functionalized gate of the

BioFET the chip can be turned into a mini-laboratory - the lab on chip. This enables better control of the environmental parameters (e.g. local pH or detecting the amount of a special protein) and gives the possibility of local measurement (e.g. how a cell reacts to a stimulus), thus providing a complete lab-on-a-chip. However, there are still many problems to overcome and a lot of research is needed. For instance, an interesting way to avoid problems by poor isolation between device and solution has been shown by (Kim et al., 2006).

## 2 METHOD

A BioFET consists of several parts: a semiconductor transducer, a dielectric layer, a biofunctionalized surface, and the analyte (Figure 1). The semiconductor transducer is a conventional FET. The dielectric layer is the gate oxide, and the biofunctionalized surface contains immobilized biomolecule receptors attached, so it is able to bind the desired molecule. The analyte is in an aqueous solution. If a target molecule binds to a receptor, the local charge density at the surface changes and thus the potential in the semiconductor. The conductivity of the channel of the field-effect transducer is changed.

The binding of the target with the receptor happens at the Angstrom length scale, while the semiconductor device is in the micrometer length scale. Thus a proper way of combining the semiconductor-solution interface is crucial.

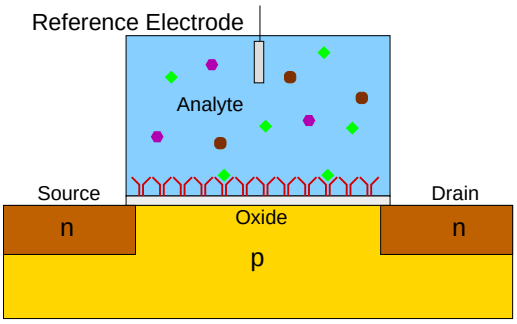


Figure 1: Schematic diagram of a BioFET.

Transport in a FET with a gate length of $1\mu m$, is usually modeled via the drift-diffusion approach (Tang and Ieong, 1995), (Selberherr, 1984). The aqueous solution is described by the Poisson-Boltzmann equation.

$$\varepsilon_0 \nabla \cdot (\varepsilon_{Ana} \nabla \psi(x,y)) = -\sum_{\sigma \in S} \sigma \, q \, c_\sigma^\infty \, e^{-\sigma \frac{q}{k_B T}(\psi(x,y)-\psi_\mu)} \tag{1}$$

$k_B$ denotes Boltzmann's constant, $T$ the temperature in Kelvin, and $\sigma \in S$, where S contains the valences of the ions in the electrolyte. $\varepsilon_0$ describes the permittivity of vacuum, and $q$ the elementary charge. $\psi_\mu$ is the chemical potential. $c_\sigma^\infty$ is the ion concentration in equilibrium, while $\varepsilon_{Ana} \approx 80$ is the relative permittivity of water.

The sum describes the carrier densities arising from the Boltzmann model. Assuming sodium-chloride as salt, which is a $1:1$ salt, the expression given in (1) can be reduced to

$$\varepsilon_0 \nabla \cdot (\varepsilon_{Ana} \nabla \psi(x,y)) = 2q \, c_\sigma^\infty \, \sinh\left(\frac{q}{k_B T}(\psi(x,y)-\psi_\mu)\right). \tag{2}$$

The charge on the surface due to chemical reaction of the $H^+$ and $OH^-$ was modeled at $pH = 7$ with the site-binding model (Shinwari et al., 2006):

$$Q_{Ox} = q \, N_S \, \frac{\frac{[H^+]_b}{K_a} e^{-\frac{q}{k_B T}\Psi(x,y)} - \frac{K_b}{[H^+]_b} e^{\frac{q}{k_B T}\Psi(x,y)}}{1 + \frac{[H^+]_b}{K_a} e^{-\frac{q}{k_B T}\Psi(x,y)} + \frac{K_b}{[H^+]_b} e^{\frac{q}{k_B T}\Psi(x,y)}}. \tag{3}$$

$N_S$ denotes the surface binding site density, while $K_a$ and $K_b$ are the equilibrium constants for charging the surface positively and negatively, respectively. $[H^+]_b$ describes the positive hydrogen ion concentration of the bulk and is corrected to the activity of the hydrogen concentration by the $e^{\frac{q}{k_B T}\Psi(x,y)}$ terms.

The biomolecules are modeled in a physics-based bottom-up approach. By calculating the charge and dipole moment for a single molecule (see for example Figure 2, (Poghossian et al., 2005)), a mean charge density and a mean dipole moment density of the boundary layer is obtained. This bridges the gap between the Angstrom length scale of the biomolecules and the micrometer dimensions of the FET (Heitzinger et al., 2008a), (Heitzinger et al., 2008b), (Ringhofer and Heitzinger, 2008), (Windbacher et al., 2008).

The link between the gate oxide and the aqueous solution is realized by two interface conditions, (Heitzinger et al., 2008a), (Heitzinger et al., 2008b), (Ringhofer and Heitzinger, 2008), (Heitzinger and Klimeck, 2007),

$$\varepsilon_0 \varepsilon_{Oxid} \, \partial_y \psi(0-,x) - \varepsilon_0 \varepsilon_{Ana} \, \partial_y \psi(0+,x) = -C(x), \tag{4}$$

$$\psi(0-,x) - \psi(0+,x) = -\frac{D_y(x)}{\varepsilon_{Ana}\varepsilon_0}. \tag{5}$$

The x-axis is parallel oriented to the oxide surface, while the y-axis points into the liquid. $\psi(0-)$ describes the potential in the oxide, while $\psi(0+)$ relates to the potential in the solute. The first equation describes the jump in the field, while the second introduces a dipole moment which causes a shift of the

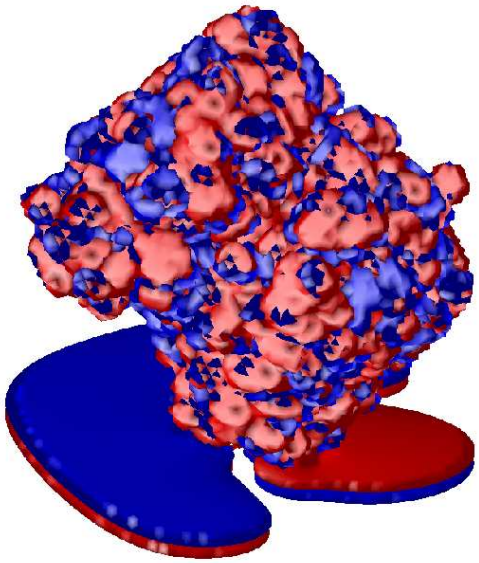

Figure 2: Biotin-streptavidin complex (http://www.pdb.org) on the oxide surface. Two iso-surfaces for plus and minus $0.03\frac{k_B T}{qA^2}$ are shown.

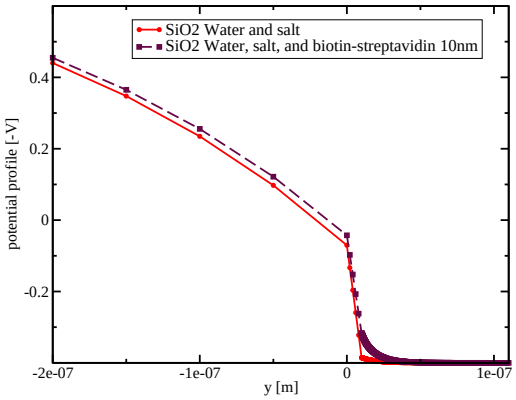


Figure 3: Potential profile at the interface (from left to right: semiconductor, oxide, solute).

potential taken into account by adjusting the potential in the analyte (Figure 3).

## 3 SIMULATION

Three different types of dielectric were simulated. $SiO_2$ as a reference, $Al_2O_3$, and $Ta_2O_5$ as possible high-k materials, with relative permitivities of 3.9, 10, and 25 respectively. As solute 1mMol sodium-chloride at pH $= 7$ was considered. The parameters for the site-binding model can be found in Table 1 (Landheer et al., 2005). For each dielectric the unprepared state (just water and salt), the prepared state (water, salt, and biotin), and the bound state when the chemical reaction has taken place (water, salt, and biotin-streptavidin) were calculated for two different mean distances between molecules ($\lambda = 10$nm, $\lambda = 15$nm). The data used for calculating charge and dipole moment of biotin and streptavidin are obtained from http://www.pdb.org (1SEW.pdb, Figures 2, 12). The potential distribution across the device is shown in Figure 4 and output curves were calculated for every parameter combination mentioned above, assuming a 100% binding efficency. The potential of the reference electrode is set to 0.4V so that the FET will be in moderate inversion as proposed by (Deen et al., 2006).

Table 1: The parameters needed for the site-binding model using different dielectric.

| Oxide | $pK_a$ | $pK_b$ | $N_S\ [cm^{-2}]$ | Reference |
|---|---|---|---|---|
| $SiO_2$ | $-2$ | 6 | $5 \cdot 10^{14}$ | (Bousse, 1982) |
| $Al_2O_3$ | 6 | 10 | $8 \cdot 10^{14}$ | (Bousse, 1982) |
| $Ta_2O_5$ | 2 | 4 | $10 \cdot 10^{14}$ | (Bousse et al., 1991) |

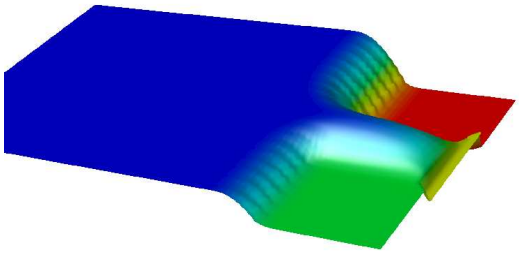

Figure 4: Potential profile for $Ta_2O_5$ water, salt, and biotin-streptavidin at $\lambda = 10$nm average distance. Blue denotes $-1$V while red stands for 1V.

## 4 RESULTS

Figures 5, 6, and 7 show a decrease in the output current for biotin attached to the surface in comparison to the unprepared surface. This downward shift for the bound state in comparison to the unbound state is due to the increase of negative charges at the interface, which is also confirmed by the difference between the curves for $\lambda = 10$nm and $\lambda = 15$nm, since for 10nm the molecules are more dense than by 15nm.

As can be seen in the Figures 5, 6, and 7 the bigger the $\varepsilon_r$ of the dielectric the bigger is the output current. Thus high-k materials deliver stronger output signals. According to (Deen, 2007) however, higher $\varepsilon_r$ dielectric constants may lead to higher trap densities and thus to a decreased signal-to-noise ratio. Therefore a trade-off between bigger output signal and signal-to-noise ratio has to be met. Figure 8 shows the output

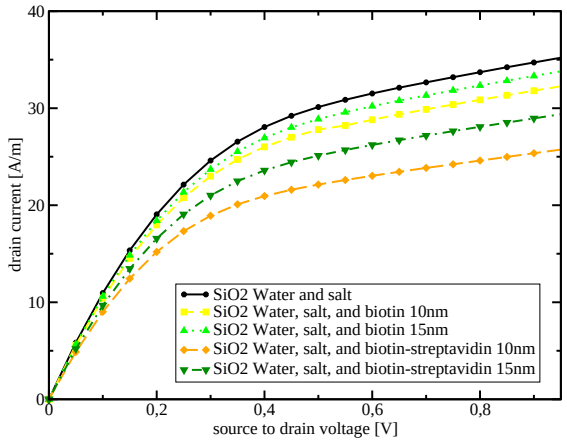


Figure 5: Output curve for $SiO_2$ for unprepared, prepared but unbound, and bound state at $\lambda = 10$nm and $\lambda = 15$nm, respectively.

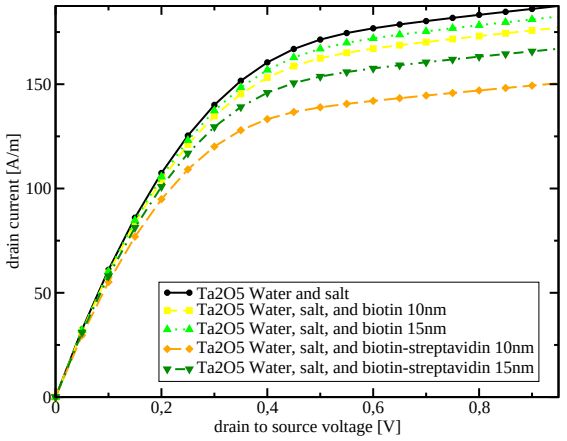


Figure 7: Output curve for $Ta_2O_5$ for unprepared, prepared but unbound, and bound state at $\lambda = 10$nm and $\lambda = 15$nm, respectively.

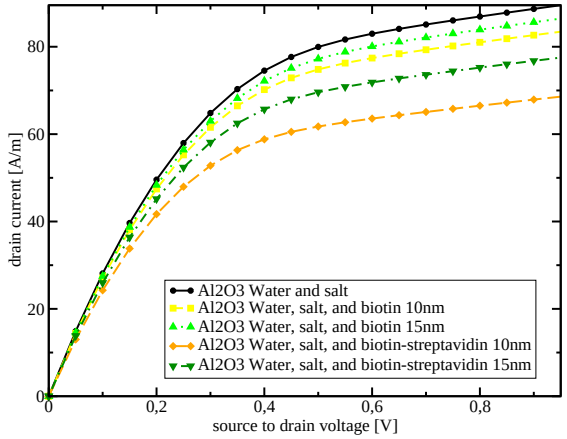


Figure 6: Output curve for $Al_2O_3$ for unprepared, prepared but unbound, and bound state at $\lambda = 10$nm and $\lambda = 15$nm, respectively.

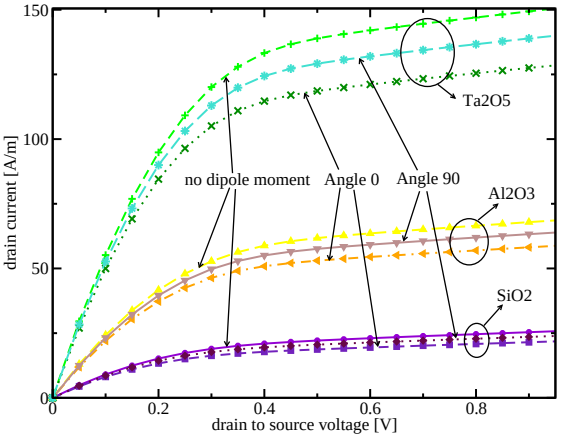


Figure 8: Output curves for $SiO_2$, $Al_2O_3$, and $Ta_2O_5$ for calculation without dipole moment, angle 0° (perpendicular to surface), and angle 90° (parallel to surface).

curves as a function of dielectric and molecule orientation (0° means perpendicular to the surface and 90° means lying flatly on the surface) leading to the lowest output curves for 0° followed by 90° and the curves without dipole moment for each group. Figures 10 and 11 show the small signal resistance as a function of dielectric and molecule orientation, displaying smaller values for higher relative permittivity $\varepsilon_r$. A slightly larger differential resistance is observed for perpendicular molecule orientation, in agreement with the previous results shown in Figures 5, 6, and 7. This is expected, because biomolecules are inhomogeneously charged. Therefore they possess a dipole moment which enters into the boundary conditions (5) and there should be a difference in the output curves of the BioFET for different orientation angles in relation to the surface.

In the biochemical community there is an ongoing discussion, if the orientation of the biomolecule is relevant for sensing. Several papers have shown contradictory results (Oh et al., 2005), (Wacker et al., 2004), (Kusnezow et al., 2003), (Peluso et al., 2003), (Turkova, 1999). All these papers are based on optical detection. Although more study is needed, we mention that for optical detection it is more important to choose the linking molecule in a way that the reaction is not hindered by steric effects (receptors block each other) or the binding sites are blocked or even broken by the crosslinker. In the case of a BioFET, however, a field-effect as working principle is used. Thus it is important to have a linker that is as short as possible, to be close to the surface. To increase the signal-to-noise ratio, the linker should have as little charge as possible. For example, in order to detect streptavidin,

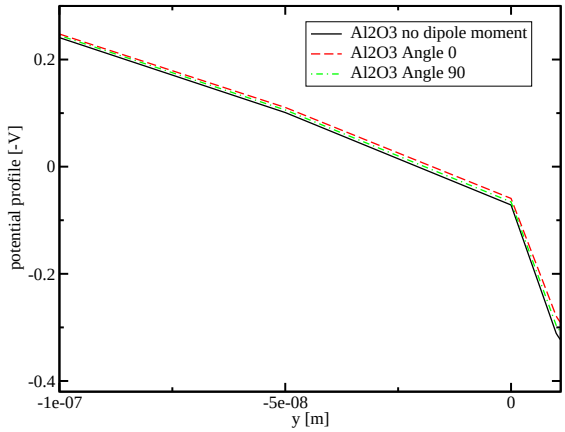


Figure 9: Potential profile for biotin-streptavidin at $\lambda =$ 10nm from left (semiconductor) to right (oxide).

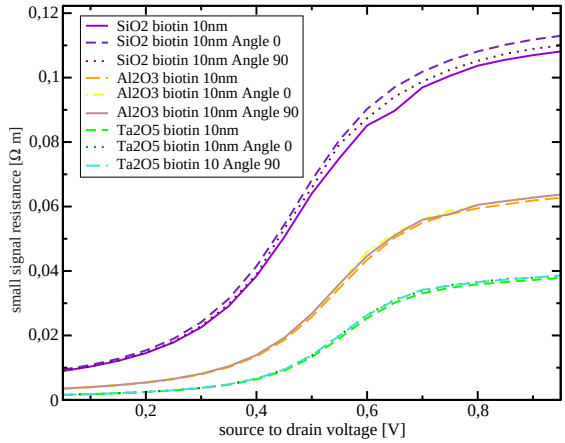


Figure 10: Small signal resistance for $SiO_2$, $Al_2O_3$, and $Ta_2O_5$ for calculation without dipole moment, angle 0° (perpendicular to surface), and angle 90° (parallel to surface) at biotin only.

biotin is used as a binding agent. A biotin molecule is attached to the surface with a neutral linker. Streptavidin then binds to biotin thus forming a bound state. The charge difference between the unbound state of a biotin alone, which is negatively charged with a single elementary charge and the bound state of biotin-streptavidin, which is negatively charged with five elementary charges, is large enough for detection. We also note that due to the tetrameric nature of streptavidin it has four sites to bind biotin as shown in Figure 12. Therefore, the linker binding biotin to the surface should be short enough in order to prevent binding several biotin molecules to a single molecule of streptavidin .

# 5 CONCLUSIONS

The model shows a strong dependence on surface charges and indicates a detectable shift in the threshold voltage depending on their orientation related to the surface. The bound state (streptavidin-biotin) negatively charged with five elementary charges compared to the unbound state (biotin) negatively charged with one elementary charge leads to a reduced conductivity, when hybridization has taken place. Also the shift of the threshold voltage and output characteristics due to different molecule orientations (0°...perpendicular to surface, 90°...lying flat on surface) can be seen. This shows the usefulness of the simulation method for the design of efficient BioFETs.

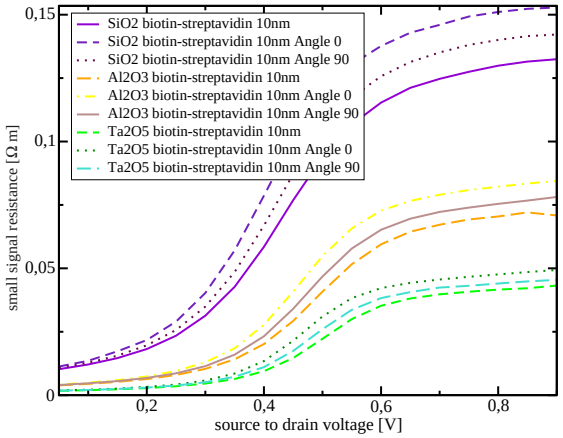


Figure 11: Small signal resistance for $SiO_2$, $Al_2O_3$, and $Ta_2O_5$ for calculation without dipole moment, angle 0° (perpendicular to surface), and angle 90° (parallel to surface) at bound state (biotin-streptavidin).

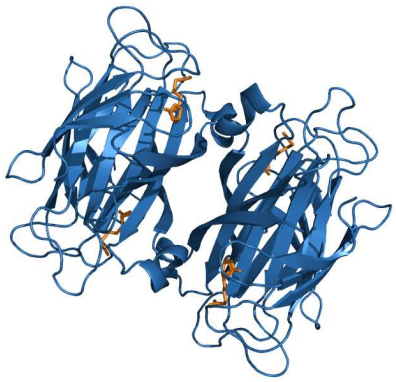

Figure 12: Scheme of the tetrameric protein streptavidin and biotin.

## REFERENCES


Bousse, L. (1982). *The Chemical Sensitivity of Electrolyte/Insulator/Silicon Structures*. PhD thesis.

Bousse, L., Mostarshed, S., Van Der Shoot, B., De Rooij, N. F., Gimmel, P., and Gopel, W. (1991). Zeta potential measurements of $Ta_2O_5$ and $SiO_2$ thin films. *Journal of Colloid and Interface Science*, 147(1):22–32.

Cui, Y., Wei, Q., Park, H., and Lieber, C. M. (2001). Nanowire nanosensors for highly sensitive and selective detection of biological and chemical species. *Science*, 293(5533):1289–1292.

Deen, M. J. (2007). Highly sensitive, low-cost integrated biosensors. In *SBCCI 2007: 20th Symposium on Integrated Circuits and System Design*, page 1.

Deen, M. J., Shinwari, M. W., Ranuárez, J. C., and Landheer, D. (2006). Noise considerations in field-effect biosensors. *Journal of Applied Physics*, 100(7):074703–1 –074703–8.

Fritz, J., Cooper, E. B., Gaudet, S., Soger, P. K., and Manalis, S. R. (2002). Electronic detection of DNA by its intrinsic molecular charge. In *PNAS*, volume 99, pages 1412–1416.

Gao, Z., Agarwal, A., Trigg, A., Singh, N., Fang, C., Tung, C., Fan, Y., Buddharaju, K., and Kong, J. (2007). Silicon nanowire arrays for label-free detection of DNA. *Analytical Chemistry*, 79(9):3291–3297.

Girard, A., Bendria, F., Sagazan, O. D., Harnois, M., Bihan, F. L., Salaün, A., Mohammed-Brahim, T., Brissot, P., and Loréal, O. (2006). Transferrin electronic detector for iron disease diagnostics. *IEEE Sensors*, pages 474–477.

Gupta, S., Elias, M., Wen, X., Shapiro, J., and Brillson, L. (2008). Detection of clinical relevant levels of protein analyte under physiologic buffer using planar field effect transistors. *Biosensors and Bioelectronics*, 24:505–511.

Hahm, J. and Lieber, C. M. (2004). Direct ultrasensitive electrical detection of DNA and DNA sequence variations using nanowire nanosensors. *Nano Letters*, 4(1):51–54.

Heitzinger, C., Kennell, R., Klimeck, G., Mauser, N., McLennan, M., and Ringhofer, C. (2008a). Modeling and simulation of field-effect biosensors (BioFETs) and their deployment on the nanoHUB. *J. Phys.: Conf. Ser.*, 107:012004/1–12.

Heitzinger, C. and Klimeck, G. (2007). Computational aspects of the three-dimensional feature-scale simulation of silicon-nanowire field-effect sensors for DNA detection. *Journal of Computational Electronics*, 6:387–390.

Heitzinger, C., Mauser, N., and Ringhofer, C. (2008b). Multi-scale modeling of planar and nanowire field-effect biosensors. submitted.

http://www.pdb.org.

Im, H., Huang, X. ., Gu, B., and Choi, Y. . (2007). A dielectric-modulated field-effect transistor for biosensing. *Nature Nanotechnology*, 2(7):430–434.

Kim, D., Park, J., Shin, J., Kim, P., Lim, G., and Shoji, S. (2006). An extended gate FET-based biosensor integrated with a Si microfluidic channel for detection of protein complexes. *Sensors and Actuators, B: Chemical*, 117:488–494.

Kusnezow, W., Jacob, A., Walijew, A., Diehl, F., and Hoheisel,J.D. (2003). Antibody microarrays: An evaluation of production parameters. *Proteomics*, 3(3):254–264.

Landheer, D., Aers, G., McKinnon, W., Deen, M., and Ranuárez, J. (2005). Model for the field effect from layers of biological macromolecules on the gates of meta-oxide-semiconductor transistors. *journal of applied physics*, 98(4):044701–1 –044701–15.

Oh, S. W., Moon, J. D., Lim, H. J., Park, S. Y., Kim, T., Park, J., Han, M. H., Snyder, M., and Choi, E. Y. (2005). Calixarene derivative as a tool for highly sensitive detection and oriented immobilization of proteins in a microarray format through noncovalent molecular interaction. *FASEB Journal*, 19(10):1335–1337.

Park, K., Lee, S., Sohn, Y., and S.Y, C. (2008). BioFET sensor for detection of albumin in urine. *Electronic Letters*, 44(3).

Peluso, P., Wilson, D. S., Do, D., Tran, H., Venkatasubbaiah, M., Quincy, D., Heidecker, B., Poindexter, K., Tolani, N., Phelan, M., Witte, K., Jung, L. S., Wagner, P., and Nock, S. (2003). Optimizing antibody immobilization strategies for the construction of protein microarrays. *Analytical Biochemistry*, 312(2):113–124.

Pirrung, M. C. (2002). How to make a DNA chip. *Angew. Chem. Int. Ed.*, 41:1276–1289.

Poghossian, A., Cherstvy, A., Ingebrandt, S., Offenhäusser, A., and Schöning, M. J. (2005). Possibilities and limitations of label-free detection of DNA hybridization with field-effect-based devices. *Sensors and Actuators, B: Chemical*, 111-112(SUPPL.):470–480.

Ringhofer, C. and Heitzinger, C. (2008). Multi-scale modeling and simulation of field-effect biosensors. *ECS Transactions*, 14(1):11–19.

Selberherr, S. (1984). *Analysis and Simulation of Semiconductor Devices*, volume Springer of *ISBN: 3-211-81800-6*.

Shinwari, M. W., Deen, M. J., and Landheer, D. (2006). Study of the elecrolyte-insulator-semiconductor field-effect transistor (EISFET) with applications in biosensor design. *Microelectronics Reliability*.

Stern, E., Klemic, J., Routenberg, D., Wyrembak, P., Turner-Evans, D., Hamilton, A., LaVan, D., Fahmy, T., and Reed, M. (2007). Lable-free immunodetection with CMOS-compatible semiconducting nanowires. *Nature Letters*, 445(1):519–522.

Tang, T.-W. and Ieong, M.-K. (1995). Discretization of flux densities in device simulations using optimum artificial diffusivity. *IEEE Transactions on Computer-Aided Design of Integrated Circuits and Systems*, 14(11):1309–1315.

Turkova, J. (1999). Oriented immobilization of biologically active proteins as a tool for revealing protein interactions and function. *Journal of Chromatography B:*

*Biomedical Sciences and Applications*, 722(1-2):11–31.

Wacker, R., Schroder, H., and Niemeyer, C. M. (2004). Performance of antibody microarrays fabricated by either DNA-directed immobilization, direct spotting, or streptavidin-biotin attachment: A comparative study. *Analytical Biochemistry*, 330(2):281–287.

Windbacher, T., Sverdlov, V., Selberherr, S., Heitzinger, C., Mauser, N., and Ringhofer, C. (2008). Simulation of field-effect biosensors (BioFETs). In *Proc. Simulation of Semiconductor Processes and Devices (SISPAD 2008)*, pages P18/1–4, Hakone, Japan.

Zheng, G., Patolsky, F., Cui, Y., Wang, W. U., and Lieber, C. M. (2005). Multiplexed electrical detection of cancer markers with nanowire sensor arrays. *Nature Biotechnology*, 23(10):1294–1301.